DOI: 10.1021/ic100037z

Inorganic Chemistry
Article

Metal-Radical Chains Based on Polychlorotriphenylmethyl Radicals: Synthesis, Structure, and Magnetic Properties

Nans Roques,[†,∥,⊥] Neus Domingo,[‡,#] Daniel Maspoch,[†,#] Klaus Wurst,[§] Concepció Rovira,[†] Javier Tejada,[‡] Daniel Ruiz-Molina,[†,#] and Jaume Veciana*[,†]

[†]*Departament de Nanociència Molecular i Materials Orgànics, Institut de Ciència de Materials de Barcelona, CSIC-CIBER/BBN, Campus de la UAB, E-08193 Bellaterra, Spain,* [‡]*Departament de Física Fonamental, Universitat de Barcelona, Diagonal 647, E-08028 Barcelona, Spain, and* [§]*Institut für Allgemeine Anorganische und Theoretische Chemie, Universitat Innsbruck, Innrain 52a, Innsbruck, Austria.* [∥]*Present Address: CNRS LCC (Laboratoire de Chimie de Coordination), 205 route de Narbonne, F-31077 Toulouse, France.* [⊥]*Present Address: Université de Toulouse, UPS, INPT LCC, F-31077 Toulouse, France.* [#]*Present Address: Centre d'Investigació en Nanociencia i Nanotecnologia (CIN2, ICN-CSIC), Campus UAB, E-08193 Bellaterra, Spain.*

Received January 7, 2010

We report the synthesis, crystal structures, and magnetic properties of two new metal-radical chains built up from a new class of organic radical-based ligands, the polychlorinated triphenylmethyl (PTM) radicals. Crystal structures of two new 1D coordination polymers, $[Cu_2(PTMDC)_2(py)_5(EtOH)]\cdot 3EtOH$ (**1**) and $[Co_2(PTMDC)_2(DMF)_2(H_2O)_6]\cdot 5DMF$ (**2**) (where PTMDC is a PTM radical functionalized with two carboxylic groups), show similar chain-like structures, in which each of the PTMDC radicals are connecting two Cu(II) or Co(II) metal ions. Therefore, from a magnetic point of view, both structures describe a magnetic chain model based on the PTMDC-M(II) unit. In this manuscript, the magnetic exchange coupling constants between both metal ions and the bridging PTM radicals have been determined. In both cases, the temperature dependence of the magnetic susceptibility reveals antiferromagnetic exchange coupling constants between the PTMDC radicals and Cu(II) ($J/k_B = -42$ K) and Co(II) ($J/k_B = -14.6$ K) ions based on the exchange Hamiltonian $H = -J\sum S_{A_i}S_{A_{i+1}}$.

Introduction

Polychlorinated triphenylmethyl (PTM) organic radicals show promise for applications ranging from optically active devices to multifunctional magnetic materials.[1,2] To date, a number of magnetic materials built up from metal ions connected through carboxylic-substituted PTM radicals have been synthesized[3−5] following the "so-called" metal-radical approach.[6−9]

*To whom correspondence should be addressed. E-mail: vecianaj@icmab.es.

(1) (a) Ratera, I.; Ruiz-Molina, D.; Vidal-Gancedo, J.; Wurst, K.; Daro, N.; Letard, J. F.; Rovira, C.; Veciana, J. *Angew. Chem., Int. Ed.* **2001**, *40*, 919. (b) Ratera, I.; Ruiz-Molina, D.; Sporer, C.; Marcen, S.; Montant, S.; Letard, J. F.; Freysz, E.; Rovira, C.; Veciana, J. *Polyhedron* **2003**, *22*, 1851. (c) Crivillers, N.; Mas-Torrent, M.; Perruchas, S.; Roques, N.; Vidal-Gancedo, J.; Veciana, J.; Rovira, C.; Basabe-Desmonts, L.; Ravoo, B. J.; Crego-Calama, M.; Reinhoudt, D. N. *Angew. Chem., Int. Ed.* **2007**, *46*, 2215. (d) Mas-Torrent, M.; Crivillers, N.; Mugnaini, V.; Ratera, I.; Rovira, C.; Veciana, J. *J. Mater. Chem.* **2009**, *19*, 1691.

(2) (a) Maspoch, D.; Ruiz-Molina, D.; Veciana, J. *J. Mater. Chem.* **2004**, *14*, 2713. (b) Minguet, M.; Luneau, D.; Lhotel, E.; Villar, V.; Paulsen, C.; Amabilino, D. B.; Veciana, J. *Angew. Chem., Int. Ed.* **2002**, *41*, 586.

(3) (a) Maspoch, D.; Ruiz-Molina, D.; Wurst, K.; Rovira, C.; Veciana, J. *Chem. Commun.* **2002**, 2958. (b) Maspoch, D.; Ruiz-Molina, D.; Vidal-Gancedo, J.; Wurst, K.; Rovira, C.; Veciana, J. *Dalton Trans.* **2004**, 1073. (c) Maspoch, D.; Domingo, N.; Ruiz-Molina, D.; Wurst, K.; Manel Hernández, J.; Lloret, F.; Tejada, J.; Rovira, C.; Veciana, J. *Inorg. Chem.* **2007**, *46*, 1627.

(4) (a) Maspoch, D.; Domingo, N.; Ruiz-Molina, D.; Wurst, K.; Vaughan, G.; Lloret, F.; Tejada, J.; Rovira, C.; Veciana, J. *Chem. Commun.* **2005**, 5035. (b) Maspoch, D.; Ruiz-Molina, D.; Wurst, K.; Rovira, C.; Veciana, J. *Chem. Commun.* **2004**, 1164.

(5) Roques, N.; Maspoch, D.; Imaz, I.; Datcu, A.; Sutter, J.-P.; Rovira, C.; Veciana, J. *Chem. Commun.* **2008**, 3160.

(6) (a) Caneschi, A.; Gatteschi, D.; Sessoli, R.; Rey, P. *Acc. Chem. Res.* **1989**, *22*, 392. (b) Caneschi, A.; Gatteschi, D.; Rey, P. *Prog. Inorg. Chem.* **1991**, *39*, 331. (c) Iwamura, H.; Inoue, K.; Hayamizu, T. *Pure Appl. Chem.* **1996**, *68*, 243.

(7) (a) Laugier, J.; Rey, P.; Benelli, C.; Gatteschi, D.; Zanchini, C. *J. Am. Chem. Soc.* **1986**, *108*, 6931. (b) Oshio, H.; Ito, T. *Coord. Chem. Rev.* **2000**, *198*, 329. (c) Rancurel, C.; Sutter, J. −P.; Le Hoerff, T.; Ouahab, L.; Kahn, O. *New. J. Chem.* **1999**, 1333. (d) Marvilliers, A.; Pei, Y.; Cano, J.; Vostrikova, K. E.; Paulsen, C.; Rivière, E.; Audière, J. −P.; Mallah, T. *Chem. Commun.* **1999**, 1951. (e) Field, L. M.; Lahti, P. M.; Palacio, F. *Chem. Commun.* **2002**, 636. (f) Stroh, G.; Turek, P.; Rabu, P.; Ziessel, R. *Inorg. Chem.* **2001**, *21*, 5334. (g) Inoue, K.; Iwamura, H. *J. Chem. Soc., Chem. Commun.* **1994**, 2273. (h) Inoue, K.; Iwamura, H. *Adv. Mater.* **1996**, *8*, 73. (i) Marlin, D. S.; Hill, E.; Weyhermüller; Rentschler, E.; Wieghardt, K. *Angew. Chem., Int. Ed.* **2002**, *41*, 4775.

(8) (a) Hicks, R. G.; Lemaire, M. T.; Thompson, L. K.; Barclay, T. M. *J. Am. Chem. Soc.* **2000**, *122*, 8077. (b) Barclay, T. M.; Hicks, R. G.; Lemaire, M. T.; Thompson, L. K. *Chem. Commun.* **2000**, 2141. (c) Shultz, D. A.; Vostrikova, K. E.; Bodnar, S. H.; Koo, H.-J.; Whangbo, M.-H.; Kirk, M. L.; Depperman, E. C.; Kampf, J. W. *J. Am. Chem. Soc.* **2003**, *125*, 1607. (d) Ghosh, P.; Begum, A.; Herebian, D.; Bothe, E.; Hildenbrand, K.; Weyhermüller, T.; Wieghardt, K. *Angew. Chem., Int. Ed.* **2003**, *42*, 563.

(9) (a) Pokhodnya, K. I.; Petersen, N.; Miller, J. S. *Inorg. Chem.* **2002**, *41*, 1996. (b) Gandelman, M.; Rybtchinsky, B.; Ashkenazi, N.; Gauvin, R. M.; Milstein, D. *J. Am. Chem. Soc.* **2001**, *123*, 5372. (c) Karasawa, S.; Kumada, H.; Koga, N.; Iwamura, H. *J. Am. Chem. Soc.* **2001**, *123*, 9685.

Published on Web 03/10/2010

For example, a two-dimensional sponge-like magnet, MOROF-1, can be prepared by connecting Cu(II) metal ions through tricarboxylic PTM radicals,[10] whereas the use of a hexacarboxylic PTM radical allows the synthesis of a three-dimensional Cu(II) coordination polymer.[11] All these systems have shown the ability of PTM radicals to magnetically interact with metal ions and, therefore, to enhance the magnetic dimensionality of these molecular materials in comparison with those obtained from diamagnetic organic ligands. Thus far, however, no one has investigated the strength of the magnetic exchange interactions between those PTM radicals and metal ions when these radicals are acting as bridging units between two or more metal ions. This is in part because of the structural complexity of the systems synthesized so far, and the lack of theoretical models. The first quantitative studies of the magnetic exchange interactions between PTM radicals and metal ions were done in zero-dimensional (0-D) complexes composed of two monocarboxylic PTM radicals (PTMMC) coordinated to a central metal ion, for which moderate antiferromagnetic coupling interactions in the range of −15 to −50 K were determined.[3] This study has allowed a much better understanding of the strength and character of these magnetic interactions. To go one step further and study the magnetic exchange interactions when these PTM radicals are connecting two metal ions, we have recently used a dicarboxylic-substituted PTM radical (hereafter named PTMDC)[12] to design and synthesize two coordination polymers, $[Cu_2(PTMDC)_2(py)_5(EtOH)]\cdot 3EtOH$ (**1**) and $[Co_2(PTMDC)_2(DMF)_2(H_2O)_6]\cdot 5DMF$ (**2**), with one-dimensional (1-D) chain-like structures. In these structures, the PTM radicals are connecting two Cu(II) or Co(II) metal ions. In this manuscript, we show that both structures serve as excellent models for quantitatively studying the ability of PTM radicals to propagate the magnetic interactions along an extended metal-organic framework.

Experimental Section

General Considerations. All solvents were reagent grade from SDS, and they were used as received and distilled unless otherwise indicated. All organic and inorganic reagents were of high purity grade, and they were obtained from Merck, Fluka Chemie, and Aldrich Chemical Co. The PTMDC radical was prepared following the multistep synthetic methodology previously reported.[12] Since PTM radicals are highly sensitive to visible light when they are in solution, all the crystallization processes were carried out under red light. Elemental analyses were obtained from the Servei de Anàlisi de la Universitat Autònoma de Barcelona. FT-IR spectra were obtained using a Perkin-Elmer Spectrum One spectrometer. Crystalline phase purity was checked by X-ray powder diffraction (XRPD) experiments, using a diffractometer (INEL CPS-120) of Debye−Scherrer geometry.

Synthesis of $[Cu_2(PTMDC)_2(py)_5(EtOH)]\cdot 3EtOH$ (1). A mixture of PTMDC radical (0.075 g, 0.097 mmol) and $Cu(ClO_4)_2\cdot 6H_2O$ (0.036 g, 0.097 mmol) in 13 mL of ethanol and 2 mL of water was carefully layered with a solution containing 2 mL of pyridine in 15 mL of ethanol. Slow diffusion over 25 days yielded crystals of **1** as red plates. Yield: 0.058 g (52.9%). Anal. Calcd for $C_{75}H_{49}Cl_{26}Cu_2N_5O_{12}$: C, 39.84; H, 2.18; N, 3.10. Found: C, 40.17; H, 2.07; N, 3.00. FT-IR (KBr, cm^{-1}): 2950 (w), 2920 (w), 1630 (s), 1618 (m), 1532 (w), 1488 (w), 1470 (m), 1449 (m), 1377 (m), 1324 (s), 1314 (m), 1248 (m), 1219 (w), 1119 (m), 1049 (w), 1042 (w), 917 (w), 874 (w), 760 (m), 718 (w), 697 (m), 676 (m) 620 (w), 578 (w), 544 (w), 525 (w).

Synthesis of $[Co_2(PTMDC)_2(DMF)_2(H_2O)_6]\cdot 5DMF$ (2). A mixture of PTMDC radical (0.075 g, 0.097 mmol) and $Co(O_2CMe)_2\cdot 4H_2O$ (0.024 g, 0.097 mmol) in 13 mL of ethanol and 2 mL of water was carefully layered with a solution containing 2 mL of pyridine in 15 mL of ethanol. Slow diffusion over 10 days yielded a dark red solid, which was filtered off and dissolved in 10 mL of DMF. The resulting dark red solution was filtered and left undisturbed to evaporate slowly. After 60 days, dark red needle-like crystals of coordination polymer **2** were obtained. Yield: 0.043 g (38.6%). Anal. Calcd for $C_{63}H_{61}Cl_{26}Co_2N_7O_{21}$: C, 33.02; H, 2.68; N, 4.28. Found: C, 33.31; H, 2.88; N, 4.21. FT-IR (KBr, cm^{-1}): 2948 (w), 2856 (w), 1675 (s) 1614 (s), 1600(m), 1464 (m), 1403 (s), 1349 (m), 1328 (m), 1258 (m), 1109 (s), 1072 (s), 1022 (w), 839 (w), 735 (w), 727 (s), 706 (w), 672 (w), 633 (w), 627 (m), 579 (w), 521 (w).

Table 1. Crystal Data and Structure Refinement for **1** and **2**

	1	**2**
formula	$C_{75}H_{49}Cl_{26}Cu_2N_5O_{12}$	$C_{63}H_{61}Cl_{26}Co_2N_7O_{21}$
fw	2260.97	2291.75
cryst syst	triclinic	monoclinic
space group	$P\bar{1}$	$P2_1/c$
a (Å)	8.793(1)	31.532(5)
b (Å)	17.170(2)	9.263(2)
c (Å)	23.846(4)	16.646(2)
α (deg)	72.657(5)	90
β (deg)	89.696(6)	94.630(9)
γ (deg)	80.093(7)	90
V (Å^3)	3381.2(8)	4846.1(14)
Z	1	2
ρ_{calcd} (g cm^{-3})	1.110	1.571
λ (Å)	0.71073 (Mo Kα)	0.71073 (Mo Kα)
μ (mm^{-1})	0.869	1.124
T (K)	293(2)	233(2)
GOF	1.044	1.105
R^a ($I > 2\sigma(I)$)	0.1065	0.1495
$R_w{}^b$ ($I > 2\sigma(I)$)	0.2668	0.3460

$^aR = \sum||F_o| - |F_c||/\sum|F_o|$. $^bR_w = [(\sum w(|F_o| - |F_c|)^2/\sum wF_o{}^2)]^{1/2}$.

X-Ray Crystal and Molecular Structural Analyses. Crystal data and details of data collection are summarized in Table 1. X-ray single-crystal diffraction data for coordination polymers **1** and **2** were collected on a Nonius KappaCCD diffractometer with an area detector and graphite-monochromized Mo K_α radiation ($\lambda = 0.7106$ Å). Intensities were integrated using DENZO and scaled with SCALEPACK. Several scans in the ϕ and ω direction were made to increase the number of redundant reflections, which were averaged in the refinement cycles. This procedure replaces an empirical absorption correction. The structures were solved and refined using the SHELXTL software.

Crystals of compound **1** very quickly lose solvent molecules to give an amorphous material. Therefore, a small crystal of **1** was mounted and measured in a capillary containing the mother liquor from the reaction mixture allowing its formation. Despite this precaution, only weak diffraction was observed for 2θ values around 40°. The two five-coordinated Cu atoms (Cu(1) and Cu(2), respectively) lie nearby an inversion center and were refined with an occupancy of 0.5.[13] Concerning Cu(1), the $Cu(py)_3$ unit lies near a symmetry center, which produces a second $Cu(py)_3$ unit with an apparent Cu(1)···Cu(1a) distance close to 1.53 Å. This short distance between the disordered Cu atoms leads to nearly exact overlying of N(1)-containing

(10) Maspoch, D.; Ruiz-Molina, D.; Wurst, K.; Domingo, N.; Cavallini, M.; Biscarini, F.; Tejada, J.; Rovira, C.; Veciana, J. *Nat. Mater.* **2003**, *2*, 190.
(11) Roques, N.; Maspoch, D.; Luis, F.; Camón, A.; Wurst, K.; Datcu, A.; Rovira, C.; Ruiz-Molina, D.; Veciana, J. *J. Mater. Chem.* **2008**, *18*, 98.
(12) Maspoch, D.; Domingo, N.; Ruiz-Molina, D.; Wurst, K.; Tejada, J.; Rovira, C.; Veciana, J. *J. Am. Chem. Soc.* **2004**, *126*, 730–731.

(13) A similar disorder was observed for mononuclear complexes obtained reacting a monocarboxylic PTM with Cu(II) salts and pyridine. See ref 3b.

Table 2. Selected Bond Distances (Å), Bond Angles, and Torsion Angles (deg) for **1**[a]

bond distances		bond and torsion angles			
Cu(1)−O(1)	1.94(1)	C(2)−O(4)−O(3)−C(2)	−2(3)	O(2)#1−Cu(1)−N(2)	79(1)
Cu(1)−O(2)#1	2.11(2)	C(1)−O(1)−O(2)−C(1)	−2(5)	N(1)−Cu(1)−N(2)	110(1)
Cu(1)−N(1)	2.22(3)	C(11)−C(10)−C(9)−C(6)	42(2)	N(1)#1−Cu(1)−N(2)	109(1)
Cu(1)−N(1)#1	2.29(3)	C(17)−C(16)−C(9)−C(10)	48(2)	O(3)−Cu(2)−O(4)#2	176(1)
Cu(1)−N(2)	2.34(3)	C(5)−C(6)−C(9)−C(16)	51(2)	N(3)−Cu(2)−N(3a)#2	154(1)
Cu(2)−O(3)	2.04(2)	C(12)−C(13)−C(2)−O(3)	92(4)	O(3)−Cu(2)−O(5)	98(2)
Cu(2)−O(4)#2	1.97(2)	C(4)−C(3)−C(1)−O(1)	98(4)	O(4)#2−Cu(2)−O(5)	85(2)
Cu(2)−O(5)	2.30(7)	O(1)−Cu(1)−O(2)#1	163(1)	N(3)−Cu(2)−O(5)	97(2)
Cu(2)−N(3)	2.08(3)	N(1)−Cu(1)−N(1)#1	140(1)	N(3a)#2−Cu(2)−O(5)	109(2)
Cu(2)−N(3a)#2	2.26(3)	O(1)−Cu(1)−N(2)	84(1)		

[a]Symmetry operators: #1 = 3 − *x*, −*y*, 1 − *z* and #2 = 1 − *x*, 1 − *y*, −*z*.

pyridine ligands, which could be refined anisotropically. The coordination sphere of each Cu(1) is completed by N(2)-containing pyridine ligands, lying in opposite directions: these pyridine rings present a distorted geometry and were refined with bond restraints and isotropic displacement parameters. Cu(2) also lies near an inversion center, with $Cu(py)_2(EtOH)$ units separated by an apparent Cu(2)···Cu(2a) distance close to 2.42 Å. N(3)-containing pyridine coordinates Cu(2) with N(3) and Cu(2a) with C(32). Therefore, a 1:1 disorder was formulated with equal coordinates of N(3)═C(32a) and N(3a)═C(32). Because of this overlay, the thermal parameters are very high and all ring atoms must be refined isotropically; additionally, the isotropic displacement factor must be fixed for C(35) and C(36). The geometry of this ring was furthermore idealized by using bond restraints between all atoms. At least three EtOH solvent molecules with an occupancy around 0.5 were found and refined using isotropic displacement parameters with bond restraints. Because of the high *R* value and distorted geometry of the pyridine rings, hydrogen atoms could not be found and were omitted for the refinement.

Crystals of **2** were generally twinned, whereas the reciprocal lattices of different twin domains do not superimpose exactly. Crystal used for the measurement only show very weak diffraction for 2θ values around 40°. To improve the high *R* value, the 100 worst reflections were omitted. Co, Cl, and coordinated O atoms were refined with anisotropic displacement parameters, while all other atoms were refined with isotropic ones to reduce the parameter numbers. Two DMF molecules [C(28−30)−N(3)−O(10) and C(31−33)−N(4)−O(11)] were refined with bond restraints and a partial occupation of 0.75 for both of them. In all cases, H atoms were omitted.

Magnetic Measurements. The static magnetic susceptibilities of polycrystalline randomly oriented samples of **1** and **2** were measured in the temperature range 2−300 K with a Quantum Design MPMS superconducting SQUID magnetometer operating at a magnetic field strength of 0.3 T and 0.1 T. The paramagnetic susceptibility was calculated considering a diamagnetic correction, estimated from tabulated Pascal constants.

Results and Discussion

Synthesis. The dicarboxylic polychlorotriphenylmethyl radical PTMDC was prepared as previously described.[12] Then, a slow diffusion of an excess of pyridine in ethanol into a solution of PTMDC and $Cu(ClO_4)_2·6H_2O$ in ethanol and water yielded good-quality crystals of **1**, suitable for single crystal X-ray diffraction analysis. Attempts to obtain single crystals with other metal ions failed, despite numerous attempts with varying concentrations, solvents, and metal salts being done. Therefore, a different synthetic methodology was used to grow crystals using Co(II) metal ions. A red solid obtained thanks to the diffusion of pyridine (in ethanol) into a solution of $Co(O_2CMe)_2·4H_2O$ and PTMDC radicals (in ethanol and water) was recovered by filtration and dissolved in DMF. Slow evaporation of the resulting solution over 60 days afforded dark red crystals of complex **2**.

X-Ray Crystal Structure Description. Coordination polymer **1** crystallizes in a triclinic $P\bar{1}$ space group with two PTMDC ligands and two Cu(II) ions packed in the unit cell. Selected bond lengths (Å), bond angles, and torsion angles (deg) are reported in Table 2. Structural disorder analysis is described in the Experimental Section.

As shown in Figure 1, each PTM radical is coordinated to two different Cu(II) ions [namely, Cu(1) and Cu(2)] in a monodentate fashion. As already observed in previous examples of PTM-based Cu(II) complexes, carboxylate moieties are coordinating the metal ions in a *syn*−*syn* fashion, and they are almost coplanar.[11] The PTM unit is presenting the typical helical arrangement of the phenyl rings around the central carbon atom with torsion angles of 42, 48, and 51°, respectively. As expected, the presence of bulky chlorine atoms in the *ortho* position for each carboxylate group makes them almost orthogonal with respect to the phenyl ring to which they are bound. The two different Cu(II) ions display a square pyramidal coordination geometry by binding two pyridine molecules and one ethanol molecule in the case of Cu(2), whereas the coordination sphere of the Cu(1) ion is completed by three pyridine ancillary ligands. This repetitive unit propagates in the [2 −1 1] direction to generate infinite corrugated chains (Figure 2a), where consecutive PTM molecules are presenting opposite helicities (*plus* and *minus*). These chains are interacting through Cl···Cl contacts (Cl(12)···Cl(2), two per PTM radical) to form honeycomb-like grids (Figure 2b). Packing of the grids along the *a* direction *via* similar contacts (Cl(4)···Cl(5) and Cl(10)···Cl(13), 4 per PTM radical) generates the overall structure that reveals cross-like channels (Figure S1 in the Supporting Information).

These channels are filled with ethanol solvent molecules. Overall, the structure of **1** can be described as an analogous structure to that shown by MOROF-1.[10] The main difference between both structures is that the $-CO_2-Cu-O_2C-$ coordination bonds that connect the chains and form the coordinating layers in MOROF-1 are replaced by weaker Cl···Cl short contacts in **1**. These observations contribute to an explaination of the "crystal to amorphous" transformation when crystals of **1** are removed from their mother liquor. Nevertheless, in the present case, this transformation is not reversible, likely

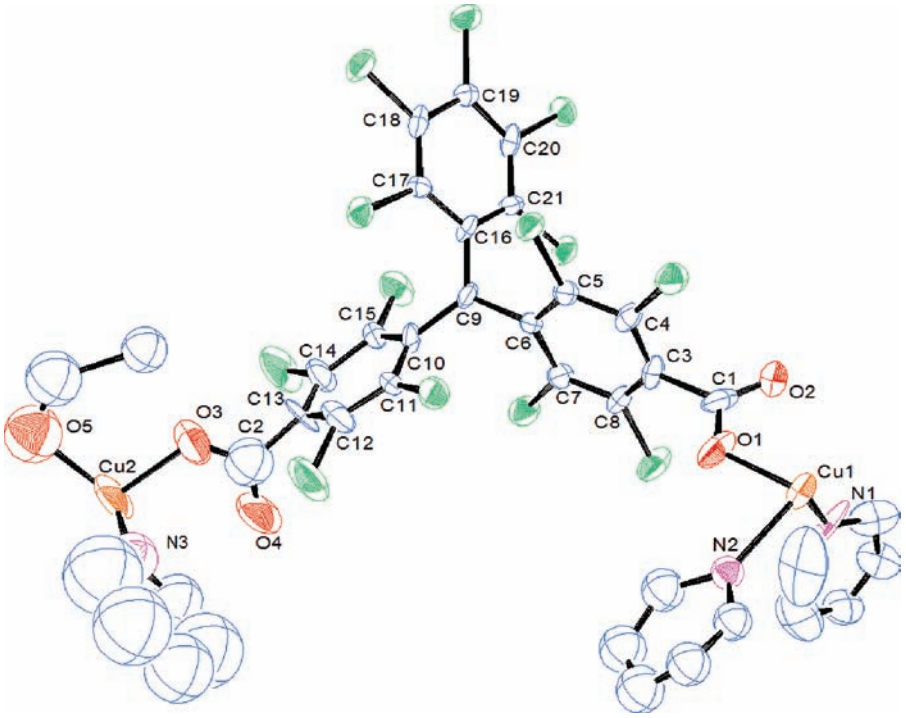

Figure 1. ORTEP drawing for coordination polymer **1** at the 25% probability level (noncoordinated solvent molecules are omitted for clarity; C, blue; Cl, green; O, red; N, pink; Cu, orange).

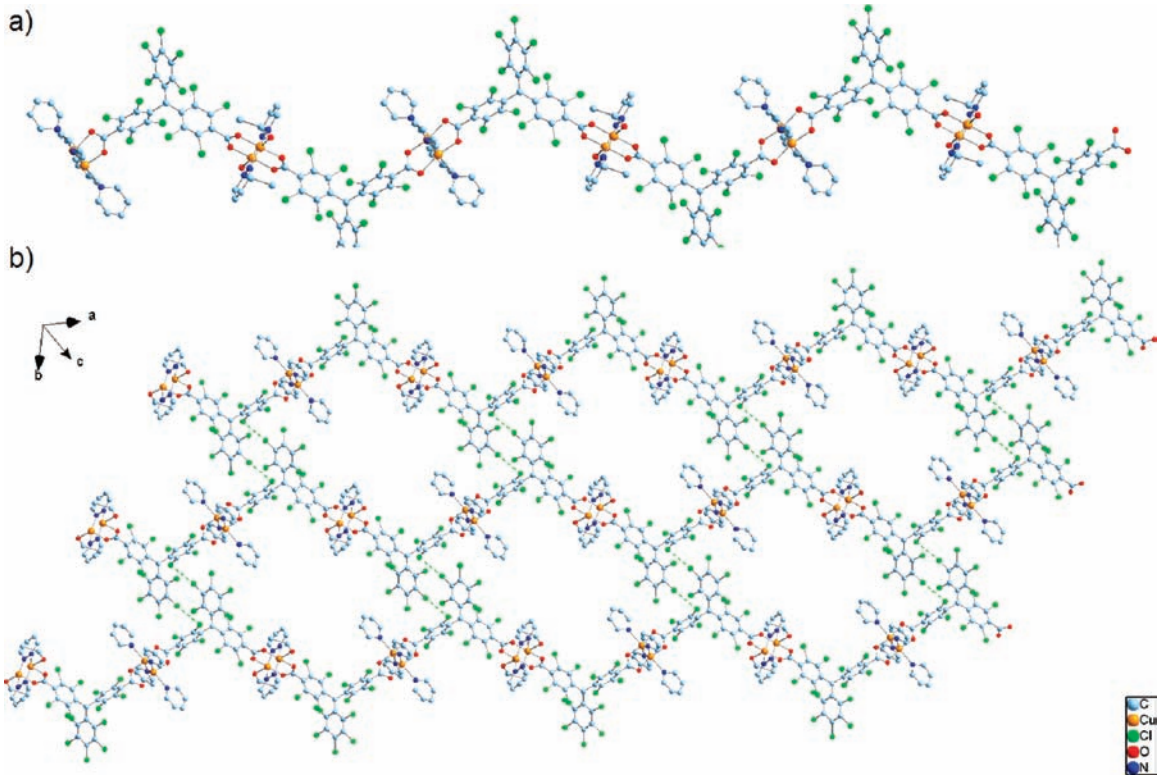

Figure 2. Structure of $[Cu_2(PTMDC)_2(py)_5(EtOH)]\cdot 3EtOH$ (**1**). (a) Chain-like structure resulting from the connection of Cu(II) ions through PTMDC units and (b) Cl···Cl short contacts (dashed green lines) yield to the formation of supramolecular grids (Cu (II) ions −orange spheres− are disordered over two positions with a 0.5 occupancy; guest ethanol solvent molecules are omitted for clarity).

because solvent departure creates much more disorder than in MOROF-1.[10]

A chain-like architecture is also observed in **2**. This coordination polymer crystallizes in a monoclinic $P2_1/c$ space group with two PTMDC molecules and two Co(II) ions packed in the unit cell. Both Co(1) and Co(2) are placed in symmetry centers, and they are octahedrally coordinated by two monodendate PTM radicals and four

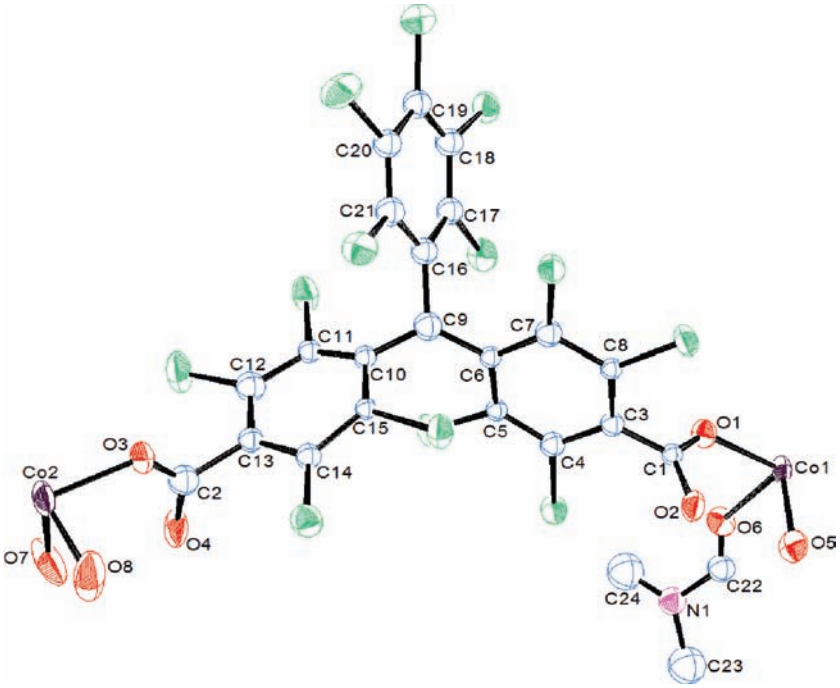

Figure 3. ORTEP drawing for coordination polymer **2** at the 25% probability level (noncoordinated solvent molecules are omitted for clarity; C, blue; Cl, green; O, red; N, pink; Co, violet).

Table 3. Selected Bond Distances (Å), Bond Angles, and Torsion Angles (deg) for **2**[a]

bond distances		bond and torsion angles			
Co(1)−O(1)	2.08(2)	C(1)−O(1)−O(1)−C(1)	180	O(1)−Co(1)−O(5)	90.0(7)
Co(1)−O(5)	2.10(2)	C(2)−O(3)−O(3)−C(2)	180	O(1)−Co(1)−O(6)	91.0(9)
Co(1)−O(6)	2.08(2)	C(15)−C(10)−C(9)−C(6)	48(4)	O(5)−Co(1)−O(6)	92.0(9)
Co(2)−O(3)	2.07(2)	C(21)−C(16)−C(9)−C(10)	48(4)	O(3)−Co(2)−O(3)#2	180.0(4)
Co(2)−O(7)	2.04(3)	C(7)−C(6)−C(9)−C(16)	48(4)	O(7)−Co(2)−O(7)#2	180.00(1)
Co(2)−O(8)	2.03(3)	C(4)−C(3)−C(1)−O(1)	98(4)	O(8)−Co(2)−O(8)#2	180(3)
		C(14)−C(13)−C(2)−O(3)	94(4)	O(3)−Co(2)−O(7)	91(1)
		O(1)−Co(1)−O(1)#1	180.0(4)	O(3)−Co(2)−O(8)	91(1)
		O(5)−Co(1)−O(5)#1	180.0(9)	O(7)−Co(2)−O(8)	90(2)
		O(6)−Co(1)−O(6)#1	180.0(3)		

[a]Symmetry operators: #1 = $1-x, 1-y, 1-z$ and #2 = $-x, 1-y, 1-z$.

water molecules for Co(2), and two monodendate PTM radicals, two water molecules, and two DMF molecules for Co(1) (see Figure 3). Carbonyls of each carboxylate group are interacting with coordinated water molecules through hydrogen bonds ($d_{O(4)\cdots O(7)w}$ = 2.61 Å; $d_{O(2)\cdots O(5)w}$ = 2.63 Å) in such a way that carboxylates coordinating each Co(II) ion are perfectly coplanar. While a *syn*−*syn* coordination mode was observed in **1**, these interactions are originating a *syn*−*anti* mode in **2**. Representative bond distances, bond angles, and torsion angles are reported in Table 3. As in **1**, the two PTM units are alternating *plus* and *minus* helicities, leading to racemic chains. Nevertheless, packing of the chains is performed in a completely different way.

In the *ab* plane, as shown in Figure 4b, the PTMDC−Co chains are associated through Cl···Cl short contacts (Cl(8)···Cl(10), 2 per PTM molecule) to afford corrugated layers. Packing of these supramolecular layers along the *c* direction is assumed through Cl···π contacts (Cl(12)···C(14), $d_{Cl(12)\cdots C(14)}$ = 3.31 Å, 2 per PTM molecule) and very weak H-bonds established between CH_3 groups of DMF molecules coordinated to Co(1) and O atoms of PTM molecules ($d_{C(23)DMF\cdots O(2)}$ = 3.18 Å, 2 per Co(II) ion) of chains belonging to different layers. Overall, these associations generate a 3-D structure, which presents small rectangular channels along the *c* axis (see Figure S2 in the Supporting Information). These channels are filled with guest DMF molecules, which are interacting with the framework through weak Cl···π contacts, weak Cl···H_3C or C=O_{PTM}···H_3C hydrogen bonds (with PTM molecules), and/or C=O_{DMF}···H_2O hydrogen bonds with water molecules coordinated to Co(II).

Magnetic Properties. [Cu_2(PTMDC)$_2$(py)$_5$(EtOH)]·3EtOH (1). The thermal dependence of magnetic susceptibility for complex **1** measured at H = 1000 Oe is shown in Figure 5. The $\chi_M T$ value at room temperature is 1.45 $cm^3 \cdot K \cdot mol^{-1}$, which fully agrees with the theoretical value of 1.5 $cm^3 \cdot K \cdot mol^{-1}$ (g = 2) expected for two uncorrelated Cu(II) ions and two PTMDC radicals with local spins $S_{Cu} = S_{PTMDC}$ = 1/2. Upon lowering the temperature, $\chi_M T$ decreases smoothly until 75 K, from where there is a more pronounced fall down to a $\chi_M T$ value of 0.2 $cm^3 \cdot K \cdot mol^{-1}$ at 1.8 K. A quantitative analysis of the thermodynamic properties of an antiferromagnetic

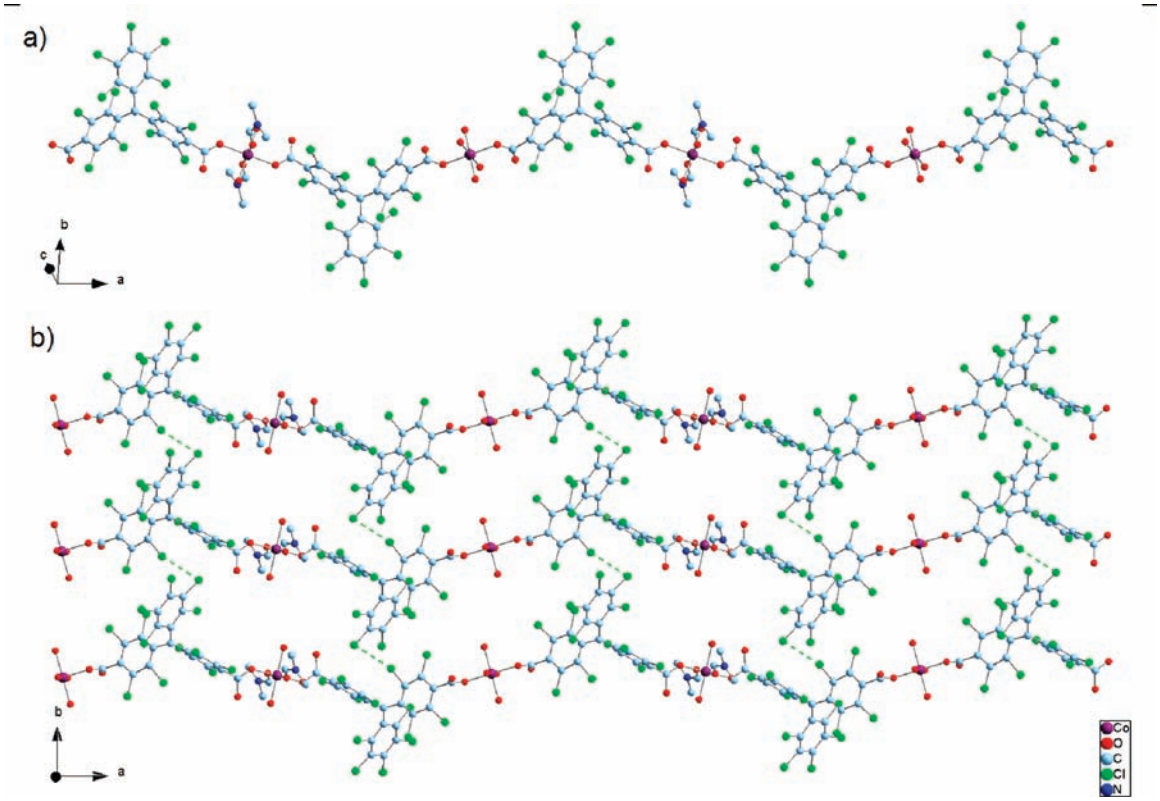

Figure 4. Structure of $[Co_2(PTMDC)_2(DMF)_2(H_2O)_6]\cdot 5DMF$ (**2**). (a) Chain-like structure resulting from the connection of Co(II) ions through PTMDC units and (b) Cl···Cl short contacts (dashed green lines) yielding to the formation of supramolecular layers (guest DMF solvent molecules are omitted for clarity).

chain of $S_A = S_B = 1/2$ is obtained considering the simplest available model for 1D systems with the spin Hamiltonian in eq 1:

$$H = -J\sum S_{A_i}S_{A_{i+1}} \qquad (1)$$

Bonner and Fisher[14] approached the magnetic susceptibility with the numerical expression (2):

$$\chi_{chain} = \frac{Ng_{eff}^2\mu_B^2}{k(T-\theta)}\frac{A + Bx + Cx^2}{D + Ex + Fx^2 + Gx^3} \qquad (2)$$

where $A = 0.25$, $B = 0.074975$, $C = 0.075235$, $D = 1.0$, $E = 0.9931$, $F = 0.172135$, and $G = 0.757825$, with $x = |J|/k_BT$. After subtracting Pascal's diamagnetism, we decomposed χ_M into[15]

$$\chi_M = \chi_{chain} + \chi_{Curie-Weiss}$$

where $\chi_{Curie-Weiss}$ represents an extrinsic Curie contribution from noninteracting spins or finite chains. The obtained expression was successfully fitted to the data with $J/k_B = -50.8 \pm 0.9$ K, $g_{eff} = 2.07 \pm 0.01$, $\theta = -0.63 \pm 0.06$ K, and a Curie constant for the paramagnetic contribution of $C = 0.28 \pm 0.01$ emu·mol^{-1}, with $R^2 = 0.99983$. In this case, the value for the antiferromagnetic interaction is slightly higher than that observed for a related 0-D Cu(II) complex, formed by an octahedral Cu(II) metal ion coordinated by two monodentated PTMMC units, for which a Cu(II)–PTMMC magnetic-exchange interaction of $J/k_B = -42$ K was determined.[3] In this case, we consider that g_{eff} is an effective value coming from the different values of the Landé factor from the Cu and PTMDC units.

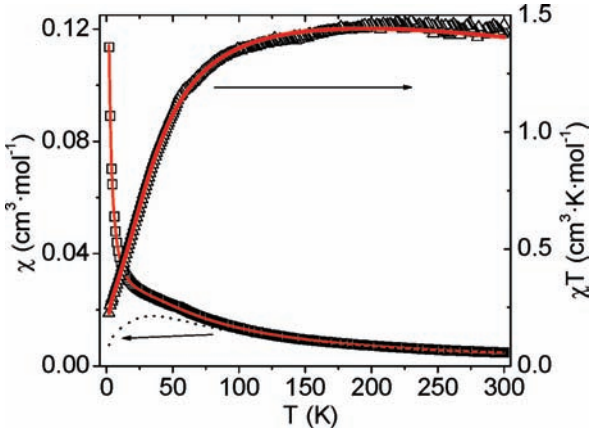

Figure 5. Thermal dependence of the magnetic susceptibility χ of complex **1** for $H = 1000$ Oe (squares) and the chain susceptibility χ_{chain} for the antiferromagnetic $S_{Cu} = S_{PTMDC} = 1/2$ chain (dot line) obtained after subtracting the Curie contribution, all referred to on the left axis. On the right axis, thermal dependence of $\chi_M T$ (triangles). The straight red lines in both cases are the fitted functions for χ_M and the corresponding $\chi_M T$ with the values in the text.

$[Co_2(PTMDC)_2(H_2O)_6(DMF)_2]\cdot 5DMF$ (2). The $\chi_M T$ vs T plot for complex **2** shown in Figure 6 exhibits all the features of ferrimagnetic chains with antiferromagnetic interchain couplings. The value of 7.08 cm^3·K·mol^{-1} at room temperature differs from the expected spin-only value of 4.5 cm^3·K·mol^{-1} expected for two octahedral high-spin Co(II) ions and two PTMDC radicals with local

(14) Bonner, J. C.; Fisher, M. E. *Phys. Rev.* **1964**, *135*, A640.
(15) Motoyama, N.; Eisaki, H.; Uchida, S. *Phys. Rev. Lett.* **1996**, *76*, 3212.

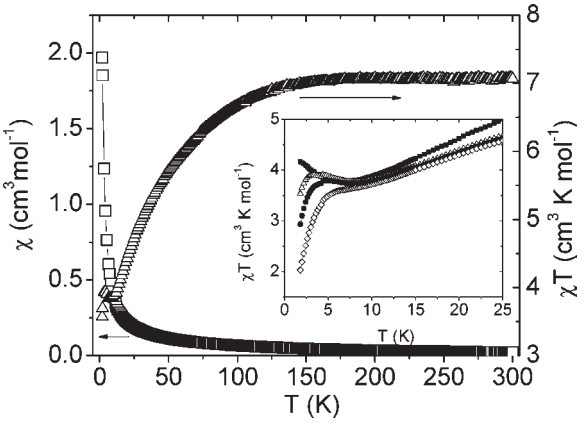

Figure 6. Thermal dependence of χ_M (squares) and the $\chi_M T$ value (triangles) for $H = 3000$ Oe, for complex **2**. The inset shows the field dependence of the low temperature maximum and the position of the minimum for $\chi_M T$, measured at $H = 500$ Oe (full square), 3000 Oe (empty triangle), 5000 Oe (full circle), and 1 T (empty diamond).

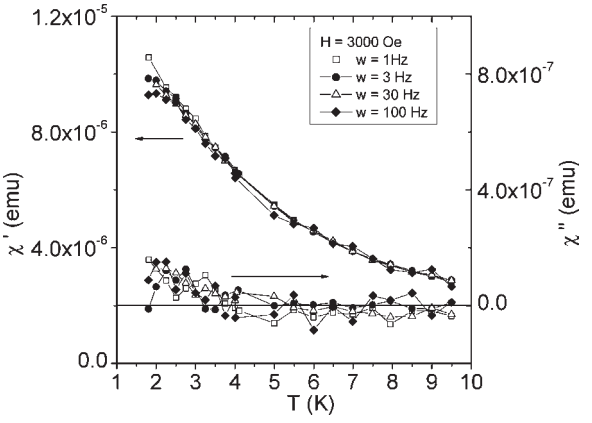

Figure 7. Thermal dependence of the magnetic ac-susceptibility at different frequencies from 1 to 100 Hz and a dc applied magnetic field of $H = 3000$ Oe, for complex **2**.

spins $S_{Co} = 3/2$ and $S_{PTMDC} = 1/2$, respectively, and isotropic Landé factor $g = 2$, implying the presence of a significant orbital contribution, arising from $L_{Co} = 1$. As the temperature is lowered, the $\chi_M T$ value decreases reaching a minimum value at 7.3 K. As temperature is further decreased, the $\chi_M T(T)$ curve increases up to a maximum at around 1.8 K, that shows saturation effects with increasing magnetic fields. The decrease of the $\chi_M T$ curve and the presence of the minimum at low temperatures is characteristic of ferrrimagnetic chains and is attributed to the presence of antiferromagnetic couplings between nearest-neighboring Co(II) ions and PTMDC radicals within the chains. In this case, one must also take into account the contribution of the depopulation of the higher energy Kramer's doublets of the Co(II) centers with a $^4T_1$ term as ground state, for the decrease of the $\chi_M T$ curve with decreasing temperature. The further increase for decreasing temperatures corresponds to the onset of long-range antiferromagnetic interactions between chains and 3-D magnetic ordering. Bulk magnetic ordering is confirmed by the presence of peaks on both, the in phase and the out of phase components of ac magnetic susceptibility, under 3K, as shown in Figure 7. On the other hand, the position of the minimum is directly related to the intensity of the antiferromagnetic interaction.[16] In the model described by van Koningsbruggen et al.,[17] for a bimetallic chain compound with half of the magnetic centers orbitally degenerated, the position of the minimum is on the order of $T_{min} \sim |J|/(2k_B)$ for a ferrimagnetic chain with $g_A \neq g_B$ and $S_A = 1/2$ and $S_B = 3/2$. From this, we obtain an estimation of $J/k_B = -14.6$ K for the interactions between Co(II) ions and PTMDC radicals in complex **2**. Even this value is a rough estimation for the interaction between the Co(II) ions and PTMDC radicals; it is in good agreement with the value $J/k_B = -15.2$ K obtained for the corresponding magnetic trimer, formed by a Co(II) ion coordinated by two monocarboxylic PTM radicals.[3] Moreover, the value of $\chi_M T_{min}$ for the ferrimagnetic Heisenberg chain of $S_A = 1/2$ and $S_B = 3/2$ is 2.221 $cm^3 \cdot K \cdot mol^{-1}$ per spin pair,[16] slightly higher than the experimental value of 1.875 $cm^3 \cdot K \cdot mol^{-1}$ obtained for $\chi_M T_{min}$ of complex **2**, for which the depopulation of the higher energy Kramer's doublets of the Co(II) centers with a $^4T_1$ term as ground state strongly decreases the effective magnetic moment in this temperature range.

Summary

We have used the PTMDC radical to design and synthesize two coordination polymers with one-dimensional (1-D) chain-like structures, in which the PTM radicals are connecting two Cu(II) or Co(II) metal ions. We have quantitatively studied the ability of PTM radicals to propagate the magnetic interactions along the extended metal-organic framework, by modeling the magnetic susceptibility of compound **1** $[Cu_2(PTMDC)_2(py)_5(EtOH)] \cdot 3EtOH$ as an antiferromagnetic chain with $S_A = S_B = 1/2$ and using the numerical expression given by Fisher and Bonner. Values of $J/k_B = -50.8 \pm 0.9$ K, $g_{eff} = 2.07 \pm 0.01$, and $\theta = -0.63 \pm 0.06$ K are obtained, slightly stronger than the exchange interaction measured for the corresponding 0D compound. On the other hand, a qualitative approach of the exchange interaction constant is obtained for compound **2** $[Co_2(PTMDC)_2(H_2O)_6(DMF)_2] \cdot 5DMF$ by analyzing the position of the minimum of the $\chi_M T$ curve, from which a value of $J/k_B = -14.76$ K is obtained, slightly lower than the exchange interaction measured for its 0D compound.

Acknowledgment. This work was supported by DGI, Spain (Project MAT2003-04699 and MAT2009-13977-C03-03) CIBER-BBN an initiative of ISCIII, and DGR Catalonia (Project 2001SGR00362). N.D. thank the Ministerio de Innovación y Ciencia for a JdC contract. D.M. thank the Ministerio de Ciencia y Tecnología for a RyC contract.

Supporting Information Available: This material is available free of charge via the Internet at http://pubs.acs.org.

(16) Drillon, M.; Coronado, E.; Georges, R.; Gianduzzo, J. C.; Curley, J. *Phys. Rev. B* **1989**, *40*, 10992.

(17) Magnetic data of complex **2** can be quantitatively described on the basis of the branch chain model previously developed in Van Kroningsbruggen Kahn, O; Nakatani, K.; Pei, Y; Renard, J. P.; Drillon, M.; Legoll, P. *Inorg. Chem.* **1990**, *29*, 3325 for a similar ferrimagnetic chain. The Hamiltonian used in this model accounts for magnetic exchange interactions between magnetic ions but also includes spin−orbit coupling effects together with the local anisotropy parameters of the Co(II) ion, and different Landée factors for each ion ($g_A \neq g_B$). Unfortunately, the proximity of the 3D magnetization ordering transition to the position of the minimum of the χT curve prevents sensible fitting of the model to our experimental data, since 3D effects could not be ignored.